



Published in final edited form as:

*Mol Psychiatry*. 2022 August ; 27(8): 3417–3424. doi:10.1038/s41380-022-01578-8.

## Serotonin Transporter Binding in Major Depressive Disorder: Impact of Serotonin System Anatomy

Elizabeth A Bartlett, PhD<sup>1,2</sup>, Francesca Zanderigo, PhD<sup>1,2</sup>, Denise Shieh, MS<sup>2,3</sup>, Jeffrey Miller, MD<sup>1,2</sup>, Patrick Hurley, MD<sup>1,2</sup>, Harry Rubin-Falcone, MS<sup>1</sup>, Maria A Oquendo, MD, PhD<sup>4</sup>, M Elizabeth Sublette, MD, PhD<sup>1,2</sup>, R Todd Ogden, PhD<sup>1,2,3</sup>, J John Mann, MD<sup>1,2,5</sup>

<sup>1</sup>Molecular Imaging and Neuropathology Area, New York State Psychiatric Institute, New York, USA

<sup>2</sup>Department of Psychiatry, Columbia University Medical Center, New York, USA

<sup>3</sup>Department of Biostatistics, Mailman School of Public Health, Columbia University Medical Center, New York, USA

<sup>4</sup>Department of Psychiatry, Perelman School of Medicine, University of Pennsylvania, Philadelphia, PA, USA

<sup>5</sup>Department of Radiology, Columbia University Medical Center, New York, USA

### Abstract

Serotonin transporter (5-HTT) binding deficits are reported in major depressive disorder (MDD). However, most studies have not considered serotonin system anatomy when parcellating brain regions of interest (ROIs). We now investigate 5-HTT binding in MDD in two novel ways: (1) use of a 5-HTT tract-based analysis examining binding along serotonergic axons; and (2) using the Copenhagen University Hospital Neurobiology Research Unit (NRU) 5-HT Atlas, based on brain-wide binding patterns of multiple serotonin receptor types. [<sup>11</sup>C]DASB 5-HTT PET scans were obtained in 60 unmedicated participants with MDD in a current depressive episode and 31 healthy volunteers (HVs). Binding potential (BP<sub>P</sub>) was quantified with empirical Bayesian estimation in graphical analysis (EBEGA). Within the [<sup>11</sup>C]DASB tract, the MDD group showed significantly lower BP<sub>P</sub> compared with HVs (p=0.02). This BP<sub>P</sub> diagnosis difference also significantly varied by tract location (p=0.02), with the strongest MDD binding deficit most proximal to brainstem

Users may view, print, copy, and download text and data-mine the content in such documents, for the purposes of academic research, subject always to the full Conditions of use: <https://www.springernature.com/gp/open-research/policies/accepted-manuscript-terms>

\* **Corresponding Author:** Elizabeth A Bartlett, PhD; eab2266@cumc.columbia.edu; 1051 Riverside Dr, New York, NY 10031.

**Author Contributions:** **EAB:** Methodology, Software, Formal Analysis, Validation, Writing – Original Draft, Visualization; **FZ:** Conceptualization, Methodology, Writing – Review & Editing, Supervision; **DS:** Formal Analysis, Data Curation, Validation, Visualization, Writing – Review & Editing; **JM:** Conceptualization, Data Curation, Investigation, Supervision, Project administration, Writing – Review & Editing; **PH:** Methodology, Writing – Review & Editing; **HRF:** Methodology, Software, Validation, Formal Analysis, Data Curation, Writing – Original Draft; **MAO:** Conceptualization, Supervision, Writing – Review & Editing; **MES:** Conceptualization, Supervision, Writing – Review & Editing, Investigation, Project Administration; **RTO:** Conceptualization, Methodology, Validation, Formal Analysis, Supervision, Writing – Review & Editing; **JJM:** Conceptualization, Investigation, Resources, Supervision, Project Administration, Funding acquisition, Writing – Review & Editing.

**Conflict of Interest:** Drs. Bartlett, Zanderigo, Miller, Hurley, Sublette, Ogden, Ms. Shieh, and Mr. Rubin-Falcone declare no conflict of interest. Drs. Oquendo and Mann receive royalties from the Research Foundation for Mental Hygiene for the commercial use of the Columbia Suicide Severity Rating Scale. Dr. Oquendo serves as an advisor to Alkermes, Otsuka, ATAI, St. George's University and Fundacion Jimenez Diaz. Her family owns stock in Bristol Myers Squibb.

raphe nuclei. NRU 5-HT Atlas ROIs showed a BP<sub>P</sub> diagnosis difference that varied by region ( $p < 0.001$ ). BP<sub>P</sub> was lower in MDD in 3/10 regions ( $p$ -values  $< 0.05$ ). Neither [<sup>11</sup>C]DASB tract or NRU 5-HT Atlas BP<sub>P</sub> correlated with depression severity, suicidal ideation, suicide attempt history, or antidepressant medication exposure. Future studies are needed to determine the causes of this deficit in 5-HTT binding being more pronounced in proximal axon segments and in only a subset of ROIs for the pathogenesis of MDD. Such regional specificity may have implications for targeting antidepressant treatment, and may extend to other serotonin-related disorders.

## Keywords

Serotonin transporter; major depressive disorder; positron emission tomography; binding patterns

---

## INTRODUCTION

Altered serotonin (5-HT) transmission has been implicated in major depressive disorder (MDD). Factors that determine serotonin signaling include serotonin neuron firing and release, receptor subtype density and affinity, and removal of serotonin from the synaptic cleft by serotonin transporters (5-HTT). Our knowledge concerning serotonin transporter density and affinity in the brain in MDD is primarily derived from postmortem work and *in vivo* imaging<sup>1</sup>. Most postmortem studies of 5-HTT binding in the brain report fewer transporters in MDD, but some studies find no difference in 5-HTT binding, in MDD relative to healthy volunteers (HVs)<sup>2,3</sup>. Similarly, most human *in vivo* imaging studies find lower<sup>4-13</sup> or similar<sup>14-17</sup> 5-HTT binding in MDD compared with HVs. However, imaging studies typically do not consider serotonergic system anatomy in choosing regions of interest (ROIs), meaning that ROIs may have heterogeneous levels of binding that degrade the binding signal obtained.

Two main anatomic circuits involved in mood regulation have been proposed, the limbic-thalamic-cortical and limbic-striatal-pallidal-thalamic-cortical circuits<sup>18</sup>. Our group has previously reported lower 5-HTT binding potential in MDD (BP<sub>P</sub>; the ratio of specifically bound radiotracer in tissue to parent radiotracer in plasma<sup>19</sup>) in six magnetic resonance imaging (MRI)-defined ROIs (midbrain, putamen, amygdala, thalamus, hippocampus, and anterior cingulate)<sup>20</sup>, but most recently our group has found no deficit in 5-HTT in MDD (for all binding potential outcome measures) in these same regions<sup>16</sup>. PET studies of the serotonin system have generally selected ROIs because they have been implicated in the pathophysiology of MDD and because they had sufficient 5-HTT binding for reliable PET quantification<sup>20,13</sup>. Moreover, traditional region definitions, e.g., Brodmann Areas, do not conform to serotonin system anatomy. Therefore, these ROIs can contain heterogeneous distributions of serotonin receptors and the transporter, potentially adding noise to data from regions with mixtures of binding levels, thereby creating the potential to miss serotonin-specific pathogenesis.

To identify serotonin-specific dysfunction in MDD, we analyzed [<sup>11</sup>C]DASB PET 5-HTT binding potential<sup>21</sup> in two ways in 60 unmedicated patients with MDD in a current depressive episode and 31 HVs. We examined: 1. [<sup>11</sup>C]DASB binding potential along the

general serotonin axonal tract originating in raphe nuclei serotonin neuron cell bodies, projecting upward to the base of the brain, forward to the frontal pole, and then sweeping back to the occipital pole; and 2. Using the Copenhagen University Hospital Neurobiology Research Unit (NRU) 5-HT Atlas, a set of brain-wide regions based on binding patterns of multiple serotonin targets in the human brain<sup>22, 23</sup>. Our hypothesis was that the lower [<sup>11</sup>C]DASB binding potential in unmedicated MDD compared with HVs would show a pattern of difference related to serotonin system anatomy that would not be detectable using general Brodmann Area-related ROIs<sup>24, 25</sup>. In the MDD group, we also examined relationships of 5-HTT binding potential with depression severity, suicide attempt history and suicidal ideation<sup>2, 26, 27</sup>.

## METHODS

### Participants

The data from all currently depressed participants with MDD (n=60) and HVs (n=31) in this analysis were compiled from subsets of these subjects in previously published studies<sup>16, 28–30</sup>. As described<sup>16, 28–30</sup>, written informed consent was obtained and the Institutional Review Board of the New York State Psychiatric Institute and Columbia University Medical Center approved the study.

MDD participant inclusion criteria included: 1) current major depressive episode; 2) 17-item Hamilton Depression Rating Scale (HDRS) score  $\geq 16$  at screening; 3) 18–65 years; 4) off all psychotropic and other types of drugs likely to interact with 5-HTT for  $\geq 14$  days at time of scan. HV inclusion criteria included: 1) absence of current or past DSM-IV Axis I diagnosis, with the exception of specific phobia, 2) absence of cluster B personality diagnosis as assessed using the SCID-II<sup>31</sup>, 3) 18–65 years. MDD and HV inclusion/exclusion criteria details are listed in Supplemental Information.

The Beck Depression Inventory (BDI)<sup>32</sup> and HDRS-17<sup>33</sup> were used to assess depression severity. The Columbia Suicide History Form<sup>34</sup> and the Scale of Suicidal Ideation<sup>35</sup> were used to assess suicide attempt history suicidal ideation, respectively.

### PET Acquisition, Processing and Quantification

Details are provided in Supplemental Information and summarized here. [<sup>11</sup>C]DASB was synthesized and scans were conducted as previously described on an ECAT HR+ scanner (Siemens/CTI, Knoxville, TN, USA)<sup>36,28</sup>. A polyurethane head holder system (Soule Medical, Tampa, FL, USA) was molded around each participant's head for immobilization purposes. Each subject received a bolus of radiotracer over 30 seconds ( $16.16 \pm 2.31$  mCi) and underwent a 10-minute transmission scan, followed by 100-minute emission scan binned into 19 frames of increasing duration. Images were reconstructed via filtered back projection with a  $128 \times 128$  matrix<sup>28</sup>. For arterial input function determination, arterial sampling was performed (automated every 10 seconds for the first 2 minutes and manually at increasing durations thereafter) to obtain arterial plasma radioactivity measurements throughout the scan and unmetabolized parent fractions at six discrete points (2, 12, 20, 50, 80, and 100 minutes via high-performance liquid chromatography)<sup>28</sup>.

Validated pre-processing was performed, including motion-correction (via registration to the eighth frame using the FMRIB linear image registration tool (FLIRT), version 5.0 (FMRIB Image Analysis Group, Oxford, UK)) and coregistration to subject T1-weighted MRIs with FLIRT<sup>28,37</sup>. A metabolite-corrected arterial plasma input function was created as described<sup>28</sup>, and was inputted into empirical Bayesian estimation in graphical analysis (EBEGA)<sup>38</sup>, a quantification approach designed to handle noise found in PET time activity curves at the voxel level<sup>38</sup>, to obtain whole-brain, voxel-wise tracer volume of distribution ( $V_T$ ) maps. Binding potential  $BP_P$  maps were then created by subtracting brain-wide estimates of the radiotracer non-displaceable distribution volume ( $V_{ND}$ ), obtained in each participant using the hybrid deconvolution approach (HYDECA)<sup>39</sup>, without having to assume any reference region.

### Definition of the Serotonin Axonal Tract

At the group level, we observed that [<sup>11</sup>C]DASB binding maps showed an arc of high binding that tracked closely with the medial serotonergic axon pathway projecting from the cell bodies in the brainstem raphe nuclei into the base of the brain, forwards to the frontal pole via the medial forebrain bundle<sup>40</sup>, and sweeping back over the cingulate to occipital cortex<sup>41</sup> (Figure 1, top). Therefore, given this observed pattern of high binding overlapped with known serotonergic system anatomy<sup>42</sup>, and the fact that depression-related pathophysiologic changes of depression tend to occur in anterior brain structures<sup>18</sup>, we sought to generate a PET-derived ROI to analyze the pattern of 5-HTT binding along this axon tract.

To generate the tract, participant MRI-derived transforms were applied to warp the  $V_T$  maps to Montreal Neurological Institute (MNI) space. The warped images were averaged across participants (Figure 1, top) and thresholded at  $V_T=11.5$ , a value chosen empirically to include the observed high binding areas overlapping with the core medial serotonergic pathway. To examine the core trajectory of serotonin axons projecting from the raphe nuclei to the occipital cortex, the medial 20 voxels were selected. Projections to regions adjacent to the axon tract like thalamus, basal ganglia, cerebellum and the cortical mantle were excluded because our focus was on the core medial axon tract<sup>41</sup>. Although axons fan out from this tract to subcortical areas and the entire cortical mantle, we sought to sample from origin to terminus, such that each axon tract segment is more distal than its previous adjacent segment (Figure 1). The resulting serotonin axonal tract was then binarized to create a single ROI (Figure 1, middle).

To analyze the pattern of 5-HTT binding potential along the tract, the binary tract was parcellated as follows (see flowchart in Supplemental Figure 1). The center sagittal slice was isolated and voxels on the border of the tract were retained. Starting at the origin in the raphe nuclei, a line was drawn through the first voxel to connect it with the voxels on the border directly surrounding it. Then, a line normal to that line was projected through the center of the tract to the opposite border, which created the dividing line between the first and second parcel. To ensure adequate estimation of binding potential in each parcel along the tract, we set the minimum volume to 100 voxels. If there were 100 voxels when the parcel was extended from the center sagittal slice to all slices in the tract, the parcel was

finalized. If there were <100 voxels, the next voxel on the tract border was considered and the line-drawing procedure (steps 4a & 4b, Supplemental Figure 1) was repeated for the parcel at hand. This was iterated until all parcels were finalized through the occipital cortex terminus. This resulted in 56 parcels, 100–400 voxels in size (Figure 1, bottom).

### Serotonin Axonal Tract Statistics

To test our *a priori* hypothesis of lower 5-HTT BP<sub>P</sub> in MDD that varies as a function of axonal tract location, we first analyzed the entire tract as a single ROI (i.e., participant-wise average BP<sub>P</sub> across all voxels in the tract) and compared diagnoses with two-tailed t-tests and linear regression (also considering age and sex).

Next, we computed BP<sub>P</sub> within each parcel along the tract, considering the observations along the tract as (nearly) continuous and applying principles of functional data analysis<sup>43</sup>. The estimated 5-HTT BP<sub>P</sub> pattern for each participant was represented as a function of distance along the tract. Using these participant-level estimates, the mean difference between MDD and HV groups was estimated at each point along the tract. To test for a main effect (consistent along the tract) of diagnostic group, the test statistic was the absolute value of the integrated difference of group mean functions. The significance of this measure was assessed based on 1,000 random permutations of group labels. To determine whether effect of diagnostic group was constant along the tract (a “pure” main effect) or if it varied as a function of location along the tract, equivalent to a test for interaction between diagnosis and tract location, the test statistic was the integrated squared difference between the two mean functions, after adjusting for the estimated main effect. Significance was based on 1,000 random permutations of group labels. The above analyses were then repeated controlling for both age and sex, and repeated only within the MDD group to explore relationships with depression severity (HDRS-17 and BDI), suicide attempt history, and history of suicidal ideation.

### NRU 5-HT Atlas Processing

To obtain ROIs with uniform 5-HTT BP<sub>P</sub>, we used the NRU 5-HT Atlas (<https://xtra.nru.dk/FS5ht-atlas/>)<sup>22, 23</sup>. This atlas, created by clustering maps of PET binding to 5-HTT and 5-HT 1A, 1B, 2A, and 4 receptors, offers 10 brain regions with homogeneous distributions of serotonin system components<sup>23</sup>. The NRU 5-HT Atlas is provided as FreeSurfer *fsaverage* overlays<sup>22, 23</sup>. Each participant’s BP<sub>P</sub> map in individual MR-space was resampled onto the *fsaverage* surface using FreeSurfer 7.1.1 reconstruction stream (<http://surfer.nmr.mgh.harvard.edu/>) run for their T1-weighted MRIs. Average BP<sub>P</sub> was extracted for the 10 serotonin regions (excluding negative values).

### NRU 5-HT Atlas Statistics

To borrow strength across NRU 5-HT Atlas ROIs and account for correlation among ROIs, we fit linear mixed-effects (LME) models to the ROI-level BP<sub>P</sub> estimates after logarithmic transformation, with participant as a random effect. The statistics for the NRU 5-HT Atlas paralleled that of the serotonin axonal tract. We first tested for a main effect of diagnosis i.e., a group effect that is consistent across regions. Secondly, we tested for a region-by-diagnosis interaction effect. The above modeling strategy was repeated while controlling for sex and

age and repeated to explore effects with depression severity, suicide attempt history, and suicidal ideation in the MDD group. Relevant code could be made available by request to the corresponding author and all statistics were performed in R v4.0.3<sup>44, 45</sup>.

## RESULTS

### Participants

Table 1 displays demographics and imaging characteristics. At enrollment, 23.3% of participants with MDD were antidepressant (AD) naïve, 6.7% had unknown AD exposure, 28.3% had AD exposure within 12 weeks, and 41.7% had AD exposure more than 12 weeks prior to the scan. Of those reporting lifetime history of AD types, 97.8% had exposure to serotonin reuptake inhibitors. Participants with MDD were older than HVs and were moderately depressed at enrollment. [<sup>11</sup>C]DASB injected dose did not differ by diagnosis.

### 5-HTT Binding Potential in the Serotonin Axon Tract

Average 5-HTT [<sup>11</sup>C]DASB BP<sub>P</sub> across the entire non-parcellated serotonin axonal tract (Figure 1, middle) was 27.0% lower in MDD compared with HVs ( $p < 0.001$ ). When considering the pattern of BP<sub>P</sub> along the parcellated tract (Figure 1, bottom), a main effect of diagnosis was found ( $p = 0.023$ ). As shown in Figures 2 and 3, for most locations along the tract, depressed individuals had lower 5-HTT BP<sub>P</sub> compared to HVs. Figure 3 displays permutation testing results, where 95% pointwise confidence intervals show that the diagnostic group difference in 5-HTT BP<sub>P</sub> excluded a zero estimate from the origin in the raphe nuclei through the first ~25% of the tract, approximately at the anterior cingulate cortex. The tract closest to the origin of serotonergic axons had the largest deficit of 5-HTT BP<sub>P</sub> in MDD. The location with the largest diagnosis difference (Figure 3) was within the ventral tegmental area (VTA) of the midbrain, where MDD 5-HTT BP<sub>P</sub> was 20.5% lower than HVs (estimate =  $-5.52$ ). Near the occipital lobe terminus, the 5-HTT BP<sub>P</sub> group difference reached zero. A robust diagnosis difference persisted until the genu of the anterior cingulate, and then abruptly declined to a small to absent group difference thereafter until the occipital lobe terminus (Figure 3).

The pattern of 5-HTT BP<sub>P</sub> group difference significantly differed from a constant function as a function of distance from axonal origin ( $p = 0.019$ , Supplemental Figure 2). When sex and age were included, the above effects persisted (main effect of diagnosis:  $p = 0.03$  and diagnosis by location interaction:  $p = 0.018$ ).

In exploratory analyses within the MDD group, 5-HTT BP<sub>P</sub> in the tract did not associate with depression severity (HDRS-17:  $p = 0.74$  or BDI:  $p = 0.47$ ), suicide attempt history ( $p = 0.44$ ), or suicidal ideation ( $p = 0.93$ ) in separate models for each variable. Also in exploratory analyses in the MDD group, 5-HTT BP<sub>P</sub> in the tract did not vary by antidepressant medication exposure across AD Naïve, AD-exposed within 12 weeks of scanning, and AD-exposed more than 12 weeks before scanning groups ( $p = 0.49$ ).

## NRU 5-HT Atlas

An example of one participant's [ $^{11}\text{C}$ ]DASB BP<sub>P</sub> map, the NRU 5-HT Atlas parcellation, and the [ $^{11}\text{C}$ ]DASB tract sampled onto the FreeSurfer *fsaverage* surface are shown in Supplemental Figure 3 for comparison.

Across all NRU 5-HT Atlas regions, a main effect of BP<sub>P</sub> across diagnoses was absent ( $F=2.50$ ,  $p=0.12$ ). When we examined the effect of brain region, we found a diagnosis-by-region effect ( $F=3.81$ ,  $p<0.001$ ). Post-hoc testing by region, indicated lower 5-HTT binding potential in MDD compared with HVs in all 10 NRU 5-HT regions (Supplemental Table 1, Figure 4; indicated by negative beta estimates (range  $-0.06$  to  $-0.15$ )). The strongest effects of lower BP<sub>P</sub> in MDD were in region 2 (95% Confidence Interval (CI)=[ $-0.27$ ,  $-0.01$ ],  $p=0.04$ ), including portions of the supramarginal, superior and transverse temporal, and insular cortices, region 6 (95% CI=[ $-0.27$ ,  $-0.009$ ],  $p=0.04$ ), including portions of the superior temporal, temporal pole, entorhinal, parahippocampal, insular, rACC, and medial and lateral orbitofrontal cortices, and region 7 (95% CI=[ $-0.28$ ,  $-0.02$ ],  $p=0.03$ ), including portions of the isthmus cingulate, parahippocampal, and entorhinal cortices (Supplemental Table 1; Figure 4). When sex and age were included, the above effects persisted (main effect:  $p=0.16$  and interaction with region:  $p<0.001$ ).

In exploratory analyses within the MDD group, there were no significant relationships between BP<sub>P</sub> and depression severity (HDRS-17 or BDI), suicide attempt history, suicidal ideation, or previous antidepressant medication exposure (all  $p$ -values $>0.05$ ).

## DISCUSSION

Within the serotonin axonal tract, there was an MDD [ $^{11}\text{C}$ ]DASB BP<sub>P</sub> deficit compared with HVs ( $p=0.02$ ) and an effect of MDD deficit by tract length ( $p=0.02$ ). The MDD 5-HTT deficit was strongest in the tract most proximal to the serotonin neuron cell bodies in the midbrain raphe nuclei, persisting until the genu of the anterior cingulate, and rapidly dissipating through to the tract terminus in occipital pole. We found a region-wise effect ( $p<0.001$ ). 5-HTT BP<sub>P</sub> was lower in 3/10 regions of distinct serotonergic characteristics ( $p=0.03$  to  $0.04$ ). We did not find that these deficits correlated with depression severity, suicidal ideation, or suicide attempt history.

### [ $^{11}\text{C}$ ]DASB Tract Analysis

We found 27.0% lower 5-HTT [ $^{11}\text{C}$ ]DASB BP<sub>P</sub> averaged over the entire serotonin axonal tract in MDD relative to HC, with prior findings of ~10% less 5-HTT binding in many brain regions in depression<sup>2</sup>. When we considered BP<sub>P</sub> in each parcel along the tract, as seen in Figure 3 and Supplemental Figure 2, the MDD BP<sub>P</sub> deficits were greatest toward the proximal section of the tract until the genu of anterior cingulate and dissipated thereafter (main effect of diagnosis:  $p=0.023$  and interaction of diagnosis by tract location:  $p=0.019$ ). No other such study has been published and replication of this finding is important, as is seeking an explanation of its cause. Perhaps axon transportation impairment or regulation of 5-HTT levels by low intra-synaptic serotonin levels are more pronounced in more proximal parts of serotonin projections.

A cause of lower 5-HTT binding in MDD may include gene variants such as 5-HTTLPR in the upstream regulatory region, some of whose alleles associate with less 5-HTT mRNA expression *in vitro*<sup>46, 47</sup>, including specifically in depressed suicide decedents<sup>48</sup>, but with mixed findings *in vivo*<sup>16, 49–52</sup>. Such a genomic effect in rodents was confined to the brainstem and not seen in the hippocampus<sup>53</sup>. A second related mechanism is epigenetic modification and DNA methylation effects from early adversity reducing 5-HTT binding in adulthood<sup>54</sup>. Another mechanism for deficits in 5-HTT binding is accelerated transporter internalization at the synaptic level due to less serotonin release from upregulation of 5-HT<sub>1A</sub> autoreceptors in depressed suicidal individuals<sup>55</sup>. This mechanism may be region-specific. Such 5-HTT internalization due to less serotonin release may be considered compensatory instead of causal in the pathogenesis of MDD. Finally, axonal transport of mRNA or proteins from the cell body, as exemplified by the transporter deficit, may be abnormal in MDD. The mechanisms responsible for these findings have important treatment implications.

The greatest MDD 5-HTT BP<sub>P</sub> deficit encompasses the VTA, which is the origin of the mesolimbic dopamine system, mediating reward, motivation, and adaptive behaviors<sup>56, 57, 58</sup>. The VTA dopamine neurons are richly innervated by afferent serotonin neurons originating in raphe nuclei<sup>59–61</sup>, that exert excitatory control. Conditioned place preference in rodents, a paradigm reflecting motivation and reward, was induced, and dopamine released in the nucleus accumbens by VTA activation of 5-HT neurons was subsequently blocked by VTA inactivation of serotonin and glutamate receptors<sup>62</sup>. Lower 5-HTT binding in MDD can have effects on limbic and cortical efferent systems through excitatory and inhibitory interactions with multiple neurotransmitter systems<sup>61</sup>.

### NRU 5-HT Atlas Analysis

Leveraging serotonergic system anatomy to define ROIs on the basis of more uniform serotonin component levels<sup>22, 23</sup>, we found a significant interaction of diagnosis-by-region 5-HTT binding potential.

Three of ten regions exhibited 5-HTT BP<sub>P</sub> deficits in MDD with 95% CIs that excluded a zero estimate (p-values=0.03 to 0.04). Interestingly, these regions do not overlap with the serotonin axonal tract; NRU 5-HT Atlas region 8 shows the greatest overlap with the tract (Supplementary Figure 1); however, does not include the brainstem and medial forebrain bundle areas where MDD 5-HTT deficits were greatest in the tract analysis, potentially explaining why region 8 did not reach post-hoc significance for MDD deficits. Given the relative widespread nature of the three regions with 5-HTT deficit in MDD, it is difficult to posit a neuroanatomical hypothesis for their involvement in depression pathophysiology. Meta-analyses suggest a widespread pattern of 5-HTT deficiency in depression (e.g., in the brainstem, amygdala, hippocampus, thalamus, striatum, frontal cortex, and cingulate cortex<sup>2, 3</sup>). We previously used six Brodmann area-based ROIs overlapping with these regions, selected for their history in depression pathophysiology and based on them having relatively high 5-HTT PET binding, offering a more robust measurement compared with low binding regions<sup>16</sup>. In those six Brodmann regions, Miller et al. 2013 found no difference in 5-HTT binding (outcome measures: V<sub>T</sub>/f<sub>p</sub>, BP<sub>P</sub>, BP<sub>ND</sub>, BP<sub>F</sub>) in MDD relative to HV<sup>16</sup>,



which disagreed with previous reports of low 5-HTT binding in MDD<sup>4-13</sup>. A recent study using a composite of regions overlapping with those studied in Miller et al. 2013 (amygdala, hippocampus, thalamus, striatum, and cingulate cortex) similarly found no difference in 5-HTT binding (outcome measure: BP<sub>ND</sub>) in MDD relative to HV, but did find potential state-specific 5-HTT binding increases after internet-delivered cognitive behavioral therapy in the MDD group<sup>63</sup>. However, using standard ROIs that don't necessarily account for serotonin binding patterns and homogenous binding levels might weaken the ability to detect disease-specific effects. The serotonin atlas-based ROIs used here showed a robust region-dependent 5-HTT binding deficit in MDD relative to HVs; however, no evidence was found for cross-sectional state effects of depression severity, suicidal ideation, or antidepressant exposure. Future studies should consider the potential advantage of considering anatomical binding patterns of a neurotransmitter-specific imaging agent in selecting ROIs for analyzing brain imaging data. Such techniques could be applied to longitudinal treatment studies aimed at disentangling state from trait effects.

In a meta-analysis, studies reporting higher depression severities had the largest MDD 5-HTT deficits in the amygdala; however, the authors acknowledge the exploratory nature of these analyses given the interstudy and interrater variability in scoring depression severity<sup>2</sup>. Of the five individual studies contributing to this portion of the meta-analysis, the three that actually reported depression severity correlations had null findings<sup>4, 8, 16</sup>. Given the absence of depression severity findings in this meta-analysis<sup>2</sup>, effects of depression severity on 5-HTT availability might be small, with individual studies unable to detect effects, even after considering serotonin binding patterns.

We previously found an effect of lower midbrain 5-HTT binding in suicide attempters relative to both non-attempters and HVs, and no effects in cortical areas (ventral prefrontal and anterior cingulate cortices)<sup>16</sup>. In the present study, we did not examine the midbrain as a whole, and likewise found no differences in binding in cortical regions using ROIs from the NRU 5-HT atlas between depressed attempters and non-attempters. These results are consistent with our previous findings<sup>4, 55</sup>. Our null findings of suicidal ideation on 5-HTT binding are discordant with the positive correlation between ideation and 5-HTT binding reported in a small sample of 10 MDD and 10 HV participants by Yeh et al. 2015<sup>27</sup> and thus, requires further follow-up.

### Strengths, Limitations, and Future Directions

Strengths of this study include a large sample size for an *in vivo* PET study, employing full quantification approach with an input function and ROIs based on serotonin system anatomy. A strength of the axonal tract analysis is that it only required two statistical tests to determine if a diagnosis effect was present and if it varied as a function of tract location, in contrast to voxel-level analyses employing thousands of tests and complex multiple comparisons correction techniques. There are also limitations. A larger sample size should be used for replication of these findings. The high-binding V<sub>T</sub> threshold used to generate the serotonin axonal tract was selected empirically based on binding level. This threshold could be further optimized and estimated in a data-driven manner in future work, which could even

include individualized thresholding to obtain tracts that better conform to individual-level serotonin system anatomy.

## Conclusion

Understanding the mechanisms by which the serotonin transporter plays a role in major depressive disorder onset and progression can assist prevention and treatment development. We found evidence for 5-HTT deficits in MDD in a midline serotonin axonal tract and region-specific serotonergic pathology. Such serotonin-specific anatomical specificity may offer new treatment targets in MDD.

## Supplementary Material

Refer to Web version on PubMed Central for supplementary material.

## Acknowledgements:

This work was supported by the National Institute of Mental health (P50MH090964, PI: J John Mann, MD and 5R01MH040695, PI: J John Mann, MD).

## REFERENCES

- Owens MJ, Nemeroff CB. Role of serotonin in the pathophysiology of depression: focus on the serotonin transporter. *Clin Chem* 1994; 40(2): 288–295. [PubMed: 7508830]
- Gryglewski G, Lanzenberger R, Kranz GS, Cumming P. Meta-analysis of molecular imaging of serotonin transporters in major depression. *Journal of Cerebral Blood Flow & Metabolism* 2014; 34(7): 1096–1103. [PubMed: 24802331]
- Kambeitz JP, Howes OD. The serotonin transporter in depression: Meta-analysis of in vivo and post mortem findings and implications for understanding and treating depression. *Journal of affective disorders* 2015; 186: 358–366. [PubMed: 26281039]
- Parsey RV, Hastings RS, Oquendo MA, Huang Y-y, Simpson N, Arcement J et al. Lower serotonin transporter potential in the human brain during major depressive episodes. *American Journal of Psychiatry* 2006; 163(1): 52–58. [PubMed: 16390889]
- Selvaraj S, Murthy NV, Bhagwagar Z, Bose SK, Hinz R, Grasby PM et al. Diminished brain 5-HT transporter binding in major depression: a positron emission tomography study with [11 C] DASB. *Psychopharmacology* 2011; 213(2–3): 555–562. [PubMed: 19756523]
- Malison RT, Price LH, Berman R, Van Dyck CH, Pelton GH, Carpenter L et al. Reduced brain serotonin transporter availability in major depression as measured by [123I]-2 $\beta$ -carbomethoxy-3 $\beta$ -(4-iodophenyl) tropane and single photon emission computed tomography. *Biological psychiatry* 1998; 44(11): 1090–1098. [PubMed: 9836013]
- Joensuu M, Tolmunen T, Saarinen PI, Tiihonen J, Kuikka J, Ahola P et al. Reduced midbrain serotonin transporter availability in drug-naive patients with depression measured by SERT-specific [123I] nor- $\beta$ -CIT SPECT imaging. *Psychiatry Research: Neuroimaging* 2007; 154(2): 125–131.
- Reimold M, Batra A, Knobel A, Smolka M, Zimmer A, Mann K et al. Anxiety is associated with reduced central serotonin transporter availability in unmedicated patients with unipolar major depression: a [11 C] DASB PET study. *Molecular psychiatry* 2008; 13(6): 606–613. [PubMed: 18268503]
- Staley JK, Sanacora G, Tamagnan G, Maciejewski PK, Malison RT, Berman RM et al. Sex differences in diencephalon serotonin transporter availability in major depression. *Biological psychiatry* 2006; 59(1): 40–47. [PubMed: 16139815]
- Willeit M, Praschak-Rieder N, Neumeister A, Pirker W, Asenbaum S, Vitouch O et al. [123I]- $\beta$ -CIT SPECT imaging shows reduced brain serotonin transporter availability in drug-free depressed

- patients with seasonal affective disorder. *Biological psychiatry* 2000; 47(6): 482–489. [PubMed: 10715354]
11. Lehto S, Tolmunen T, Joensuu M, Saarinen PI, Vanninen R, Ahola P et al. Midbrain binding of [123I] nor- $\beta$ -CIT in atypical depression. *Progress in Neuro-Psychopharmacology and Biological Psychiatry* 2006; 30(7): 1251–1255. [PubMed: 16644083]
  12. Nye JA, Purselle D, Plisson C, Voll RJ, Stehouwer JS, Votaw JR et al. Decreased brainstem and putamen SERT binding potential in depressed suicide attempters using [11C]-ZIENT pet imaging. *Depression and anxiety* 2013; 30(10): 902–907. [PubMed: 23526784]
  13. Cannon DM, Ichise M, Fromm SJ, Nugent AC, Rollis D, Gandhi SK et al. Serotonin transporter binding in bipolar disorder assessed using [11C] DASB and positron emission tomography. *Biological psychiatry* 2006; 60(3): 207–217. [PubMed: 16875929]
  14. Meyer JH, Wilson AA, Ginovart N, Goulding V, Hussey D, Hood K et al. Occupancy of serotonin transporters by paroxetine and citalopram during treatment of depression: a [11C] DASB PET imaging study. *American Journal of Psychiatry* 2001; 158(11): 1843–1849. [PubMed: 11691690]
  15. Meyer JH, Houle S, Sagrati S, Carella A, Hussey DF, Ginovart N et al. Brain serotonin transporter binding potential measured with carbon11-labeled dasb positron emission tomography: Effects of major depressive episodes and severity of dysfunctional attitudes. *Archives of general psychiatry* 2004; 61(12): 1271–1279. [PubMed: 15583118]
  16. Miller JM, Hesselgrave N, Ogden RT, Sullivan GM, Oquendo MA, Mann JJ et al. Positron emission tomography quantification of serotonin transporter in suicide attempters with major depressive disorder. *Biological psychiatry* 2013; 74(4): 287–295. [PubMed: 23453288]
  17. Ichimiya T, Suhara T, Sudo Y, Okubo Y, Nakayama K, Nankai M et al. Serotonin transporter binding in patients with mood disorders: a PET study with [11C](+) McN5652. *Biological Psychiatry* 2002; 51(9): 715–722. [PubMed: 11983185]
  18. Soares JC, Mann JJ. The functional neuroanatomy of mood disorders. *Journal of psychiatric research* 1997; 31(4): 393–432. [PubMed: 9352470]
  19. Innis RB, Cunningham VJ, Delforge J, Fujita M, Gjedde A, Gunn RN et al. Consensus nomenclature for in vivo imaging of reversibly binding radioligands. *Journal of Cerebral Blood Flow & Metabolism* 2007; 27(9): 1533–1539. [PubMed: 17519979]
  20. Parsey RV, Hastings RS, Oquendo MA, Huang YY, Simpson N, Arcement J et al. Lower serotonin transporter binding potential in the human brain during major depressive episodes. *Am J Psychiatry* 2006; 163(1): 52–58. [PubMed: 16390889]
  21. Frankle WG, Huang Y, Hwang D-R, Talbot PS, Slifstein M, Van Heertum R et al. Comparative Evaluation of Serotonin Transporter Radioligands 11C-DASB and 11C-McN 5652 in Healthy Humans. *J Nucl Med* 2004; 45(4): 682–694. [PubMed: 15073266]
  22. Beliveau V, Ozenne B, Strother S, Greve DN, Svarer C, Knudsen GM et al. The structure of the serotonin system: A PET imaging study. *Neuroimage* 2020; 205: 116240. [PubMed: 31600591]
  23. Beliveau V, Ganz M, Feng L, Ozenne B, Højgaard L, Fisher PM et al. A high-resolution in vivo atlas of the human brain's serotonin system. *Journal of Neuroscience* 2017; 37(1): 120–128. [PubMed: 28053035]
  24. Gryglewski G, Lanzenberger R, Kranz GS, Cumming P. Meta-analysis of molecular imaging of serotonin transporters in major depression. *J Cereb Blood Flow Metab* 2014; 34(7): 1096–1103. [PubMed: 24802331]
  25. Kambeitz JP, Howes OD. The serotonin transporter in depression: Meta-analysis of in vivo and post mortem findings and implications for understanding and treating depression. *J Affect Disord* 2015; 186: 358–366. [PubMed: 26281039]
  26. Gopaldas M, Zanderigo F, Zhan S, Ogden RT, Miller JM, Rubin-Falcone H et al. Brain serotonin transporter binding, plasma arachidonic acid and depression severity: a positron emission tomography study of major depression. *Journal of affective disorders* 2019; 257: 495–503. [PubMed: 31319341]
  27. Yeh Y-W, Ho P-S, Chen C-Y, Kuo S-C, Liang C-S, Yen C-H et al. Suicidal ideation modulates the reduction in serotonin transporter availability in male military conscripts with major depression: a 4-[18F]-ADAM PET study. *The World Journal of Biological Psychiatry* 2015; 16(7): 502–512. [PubMed: 26068129]

28. Ogden RT, Ojha A, Erlandsson K, Oquendo MA, Mann JJ, Parsey RV. In vivo quantification of serotonin transporters using [(11)C]DASB and positron emission tomography in humans: modeling considerations. *J Cereb Blood Flow Metab* 2007; 27(1): 205–217. [PubMed: 16736050]
29. Miller JM, Everett BA, Oquendo MA, Ogden RT, Mann JJ, Parsey RV. Positron emission tomography quantification of serotonin transporter binding in medication-free bipolar disorder. *Synapse* 2016; 70(1): 24–32. [PubMed: 26426356]
30. Parsey RV, Kent JM, Oquendo MA, Richards MC, Pratap M, Cooper TB et al. Acute occupancy of brain serotonin transporter by sertraline as measured by [11C]DASB and positron emission tomography. *Biol Psychiatry* 2006; 59(9): 821–828. [PubMed: 16213473]
31. First MB, Gibbon M, Spitzer RL, Williams JB, Benjamin LS. *SCID-II Personality Questionnaire*. American Psychiatric Press: Washington, D.C., 1997.
32. Beck AT, Ward CH, Mendelson M, Mock J, Erbauh J. An inventory for measuring depression. *Arch Gen Psychiatry* 1961; 4: 53–63.
33. Hamilton M A rating scale for depression. *J Neurol Neurosurg Psych* 1960; 23: 56–62.
34. Oquendo MA, Halberstam B, Mann JJ. Risk factors for suicidal behavior: the utility and limitations of research instruments. In: First MB (ed). *Standardized Evaluation in Clinical Practice*. American Psychiatric Publishing: Arlington, VA, 2003, pp 103–130.
35. Beck AT, Kovacs M, Weissman A. Assessment of suicidal intention: the Scale for Suicide Ideation. *Journal of consulting and clinical psychology* 1979; 47(2): 343. [PubMed: 469082]
36. Belanger MJ, Simpson NR, Wang T, Van Heertum R, Mann JJ, Parsey RV. Biodistribution and Radiation Dosimetry of [11C]DASB in Baboons. *Nucl Med Biol* 2004; 31(8): 1097–1102. [PubMed: 15607492]
37. Parsey RV, Slifstein M, Hwang DR, Abi-Dargham A, Simpson N, Mawlawi O et al. Validation and reproducibility of measurement of 5-HT1A receptor parameters with [carbonyl-11C]WAY-100635 in humans: comparison of arterial and reference tissue input functions. *J Cereb Blood Flow Metab* 2000; 20(7): 1111–1133. [PubMed: 10908045]
38. Zanderigo F, Ogden RT, Bertoldo A, Cobelli C, Mann JJ, Parsey RV. Empirical Bayesian estimation in graphical analysis: a voxel-based approach for the determination of the volume of distribution in PET studies. *Nuclear medicine and biology* 2010; 37(4): 443–451. [PubMed: 20447556]
39. Zanderigo F, Mann JJ, Ogden RT. A hybrid deconvolution approach for estimation of in vivo non-displaceable binding for brain PET targets without a reference region. *PloS one* 2017; 12(5): e0176636. [PubMed: 28459878]
40. Hornung J-P. The neuronatomy of the serotonergic system. *Handbook of Behavioral Neuroscience*, vol. 21. Elsevier 2010, pp 51–64.
41. Charnay Y, Léger L. Brain serotonergic circuitries. *Dialogues in clinical neuroscience* 2010; 12(4): 471. [PubMed: 21319493]
42. Törk I Anatomy of the Serotonergic System a. *Annals of the New York Academy of Sciences* 1990; 600(1): 9–34. [PubMed: 2252340]
43. Wang J-L, Chiou J-M, Müller H-G. Functional data analysis. *Annual Review of Statistics and Its Application* 2016; 3: 257–295.
44. Bates D, Mächler M, Bolker B, Walker S. Fitting linear mixed-effects models using lme4. *arXiv preprint arXiv:14065823* 2014.
45. Team RC. R: A language and environment for statistical computing. Vienna, Austria 2013.
46. Heils A, Teufel A, Petri S, Stöber G, Riederer P, Bengel D et al. Allelic variation of human serotonin transporter gene expression. *Journal of neurochemistry* 1996; 66(6): 2621–2624. [PubMed: 8632190]
47. Lesch K-P, Bengel D, Heils A, Sabol SZ, Greenberg BD, Petri S et al. Association of anxiety-related traits with a polymorphism in the serotonin transporter gene regulatory region. *Science* 1996; 274(5292): 1527–1531. [PubMed: 8929413]
48. Arango V, Underwood MD, Boldrini M, Tamir H, Kassir SA, Hsiung S-c et al. Serotonin 1A receptors, serotonin transporter binding and serotonin transporter mRNA expression in the brainstem of depressed suicide victims. *Neuropsychopharmacology* 2001; 25(6): 892–903. [PubMed: 11750182]

49. Parsey RV, Hastings RS, Oquendo MA, Hu X, Goldman D, Huang Y-y et al. Effect of a triallelic functional polymorphism of the serotonin-transporter-linked promoter region on expression of serotonin transporter in the human brain. *American Journal of Psychiatry* 2006; 163(1): 48–51. [PubMed: 16390888]
50. Güzey C, Allard P, Brännström T, Spigset O. Radioligand binding to brain dopamine and serotonin receptors and transporters in Parkinson's disease: relation to gene polymorphisms. *International Journal of Neuroscience* 2012; 122(3): 124–132. [PubMed: 22004534]
51. Reimold M, Smolka M, Schumann G, Zimmer A, Wrase J, Mann K et al. Midbrain serotonin transporter binding potential measured with [11 C] DASB is affected by serotonin transporter genotype. *Journal of neural transmission* 2007; 114(5): 635–639. [PubMed: 17225932]
52. Praschak-Rieder N, Kennedy J, Wilson AA, Hussey D, Boovariwala A, Willeit M et al. Novel 5-HTTLPR allele associates with higher serotonin transporter binding in putamen: a [11C] DASB positron emission tomography study. *Biological psychiatry* 2007; 62(4): 327–331. [PubMed: 17210141]
53. Albert PR, Benkelfat C. The neurobiology of depression—revisiting the serotonin hypothesis. II. Genetic, epigenetic and clinical studies. *The Royal Society* 2013.
54. Kinnally EL, Capitano JP, Leibel R, Deng L, LeDuc C, Haghghi F et al. Epigenetic regulation of serotonin transporter expression and behavior in infant rhesus macaques. *Genes, Brain and Behavior* 2010; 9(6): 575–582. [PubMed: 20398062]
55. Oquendo MA, Galfalvy H, Sullivan GM, Miller JM, Milak MM, Sublette ME et al. Positron emission tomographic imaging of the serotonergic system and prediction of risk and lethality of future suicidal behavior. *JAMA psychiatry* 2016; 73(10): 1048–1055. [PubMed: 27463606]
56. Wise RA. Dopamine, learning and motivation. *Nature reviews neuroscience* 2004; 5(6): 483–494. [PubMed: 15152198]
57. Kalivas PW, Nakamura M. Neural systems for behavioral activation and reward. *Current opinion in neurobiology* 1999; 9(2): 223–227. [PubMed: 10322190]
58. Oades RD, Halliday GM. Ventral tegmental (A10) system: neurobiology. 1. Anatomy and connectivity. *Brain Research Reviews* 1987; 12(2): 117–165.
59. Hervé D, Pickel VM, Joh TH, Beaudet A. Serotonin axon terminals in the ventral tegmental area of the rat: fine structure and synaptic input to dopaminergic neurons. *Brain research* 1987; 435(1–2): 71–83. [PubMed: 2892580]
60. Van Bockstaele EJ, Cestari DM, Pickel VM. Synaptic structure and connectivity of serotonin terminals in the ventral tegmental area: potential sites for modulation of mesolimbic dopamine neurons. *Brain research* 1994; 647(2): 307–322. [PubMed: 7522922]
61. Neurocircuitry of mood disorders. *Proceedings of the In Neuropsychopharmacology: The Fifth Generation of Progress* 2002. Citeseer.
62. Wang H-L, Zhang S, Qi J, Wang H, Cachope R, Mejias-Aponte CA et al. Dorsal raphe dual serotonin-glutamate neurons drive reward by establishing excitatory synapses on VTA mesoaccumbens dopamine neurons. *Cell reports* 2019; 26(5): 1128–1142. e1127. [PubMed: 30699344]
63. Svensson JE, Svanborg C, Plavén-Sigray P, Kalso V, Halldin C, Schain M et al. Serotonin transporter availability increases in patients recovering from a depressive episode. *Translational psychiatry* 2021; 11(1): 1–10. [PubMed: 33414379]
64. Hamilton M A rating scale for depression. *J Neurol Neurosurg Psychiatry* 1960; 23: 56–62. [PubMed: 14399272]

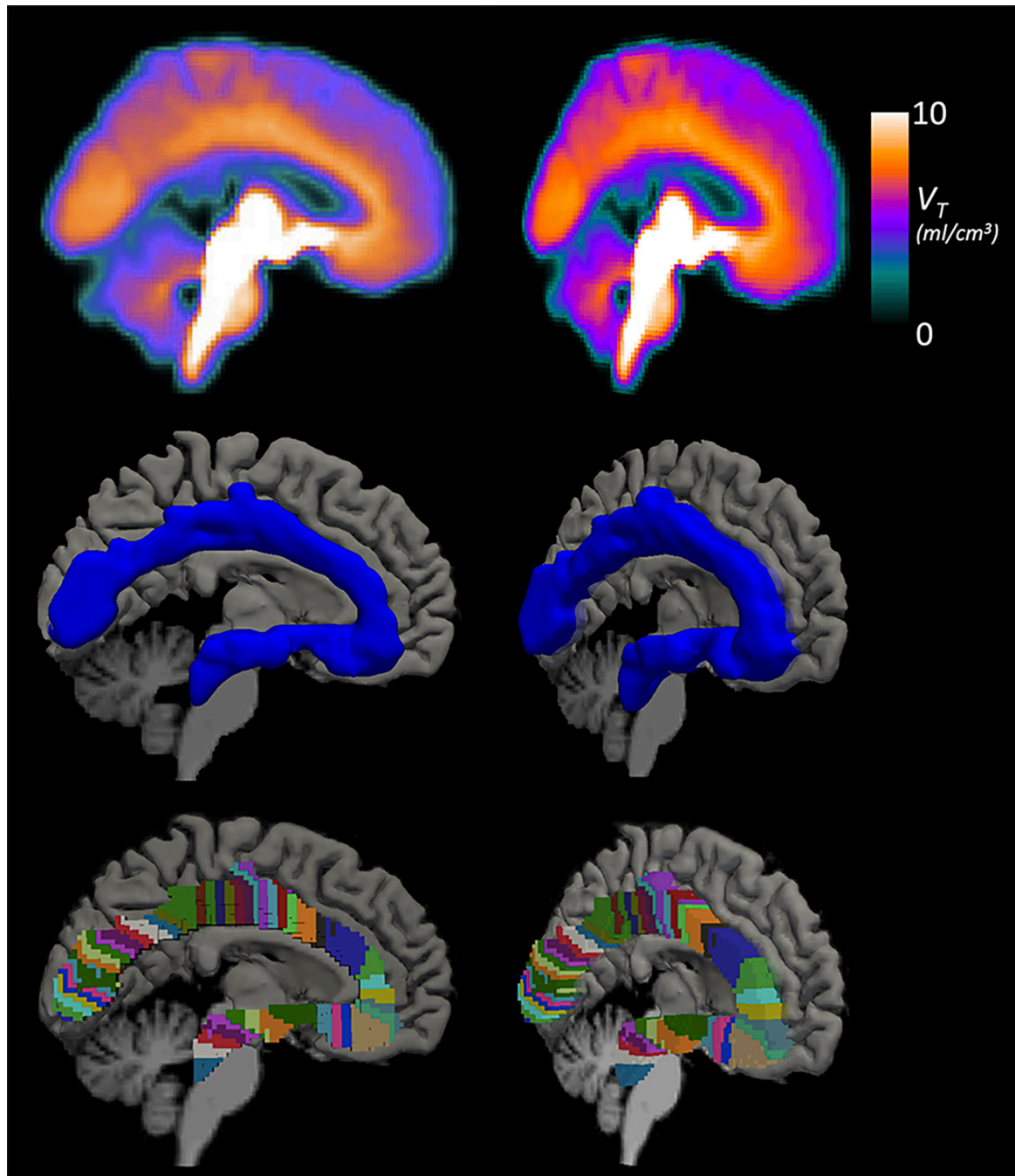


**Figure 1:**

Average volume of distribution ( $V_T$ ) across all participants (top), 3D rendering of the serotonin axonal tract in MNI space as a standard ROI (middle; blue), and the parcellated tract for analyses with the pattern of binding along the tract (bottom; multi-colored). All are shown sagittally (left) and rotated (right) to show the tract depth.

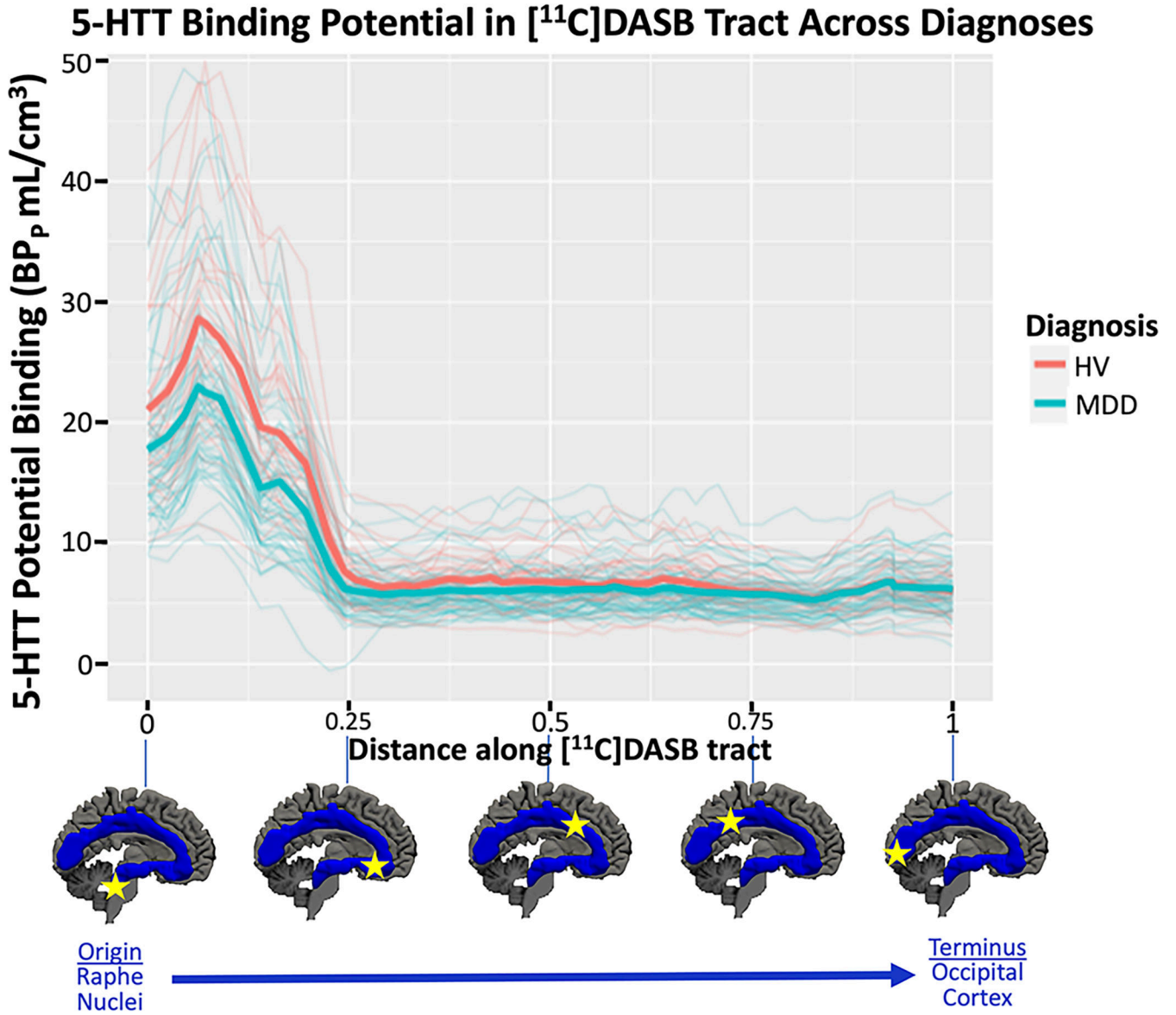


**Figure 2:** Mean [<sup>11</sup>C]DASB binding potential BP<sub>p</sub> (y-axis) in each of the 56 parcels within the serotonin axon tract plotted as a function of distance from the origin of the tract in centimeters. Diagnostic group averages plotted in thick, bold lines with HV = healthy volunteer in pink and MDD = major depressive disorder in blue. Additionally, spaghetti plots of each participant are plotted with thin lines according to their group designation. Below plot is a depiction of the x-axis regions according to their location on the tract.

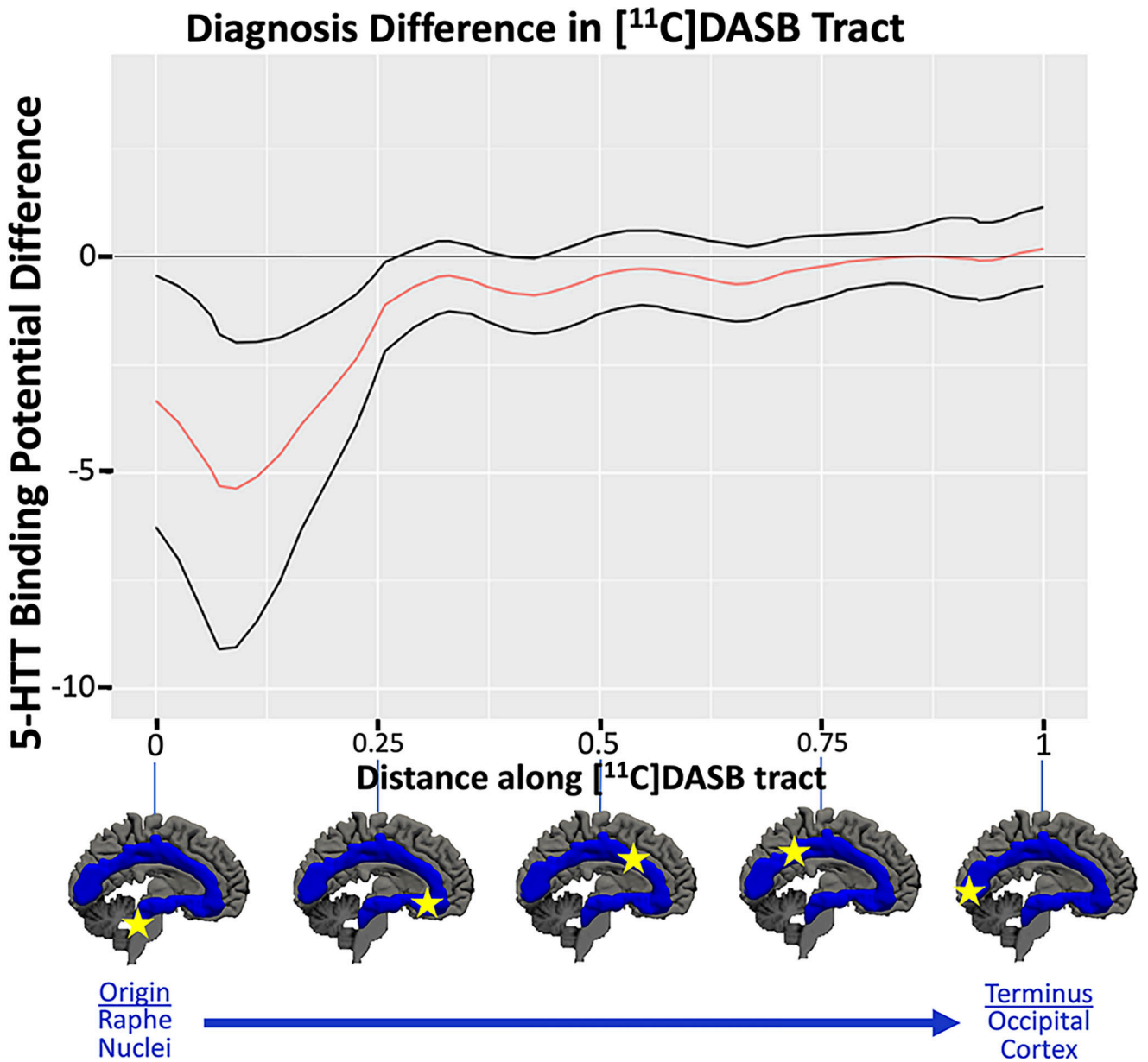


**Figure 3:**

Diagnostic group difference test: The estimated difference in 5-HTT BP<sub>P</sub> between MDD = major depressive disorder and HV = healthy volunteer groups is shown plotted against the distance along the tract. The group difference in the original dataset is plotted with a thick, solid red line. Permutation testing, examining the area under the curve for the main effect of diagnostic group yielded a p-value of 0.02. Black lines show the 95% confidence intervals obtained via bootstrapping. Locations along the tract with both confidence intervals above or below 0 indicate locations of significant group differences.



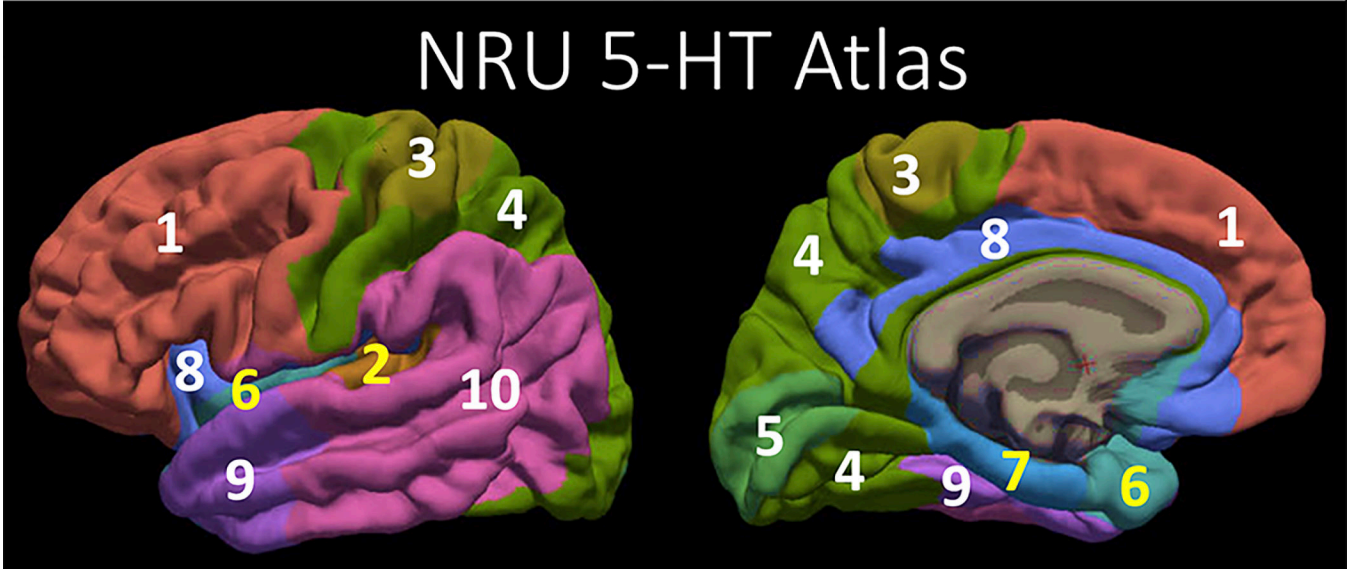
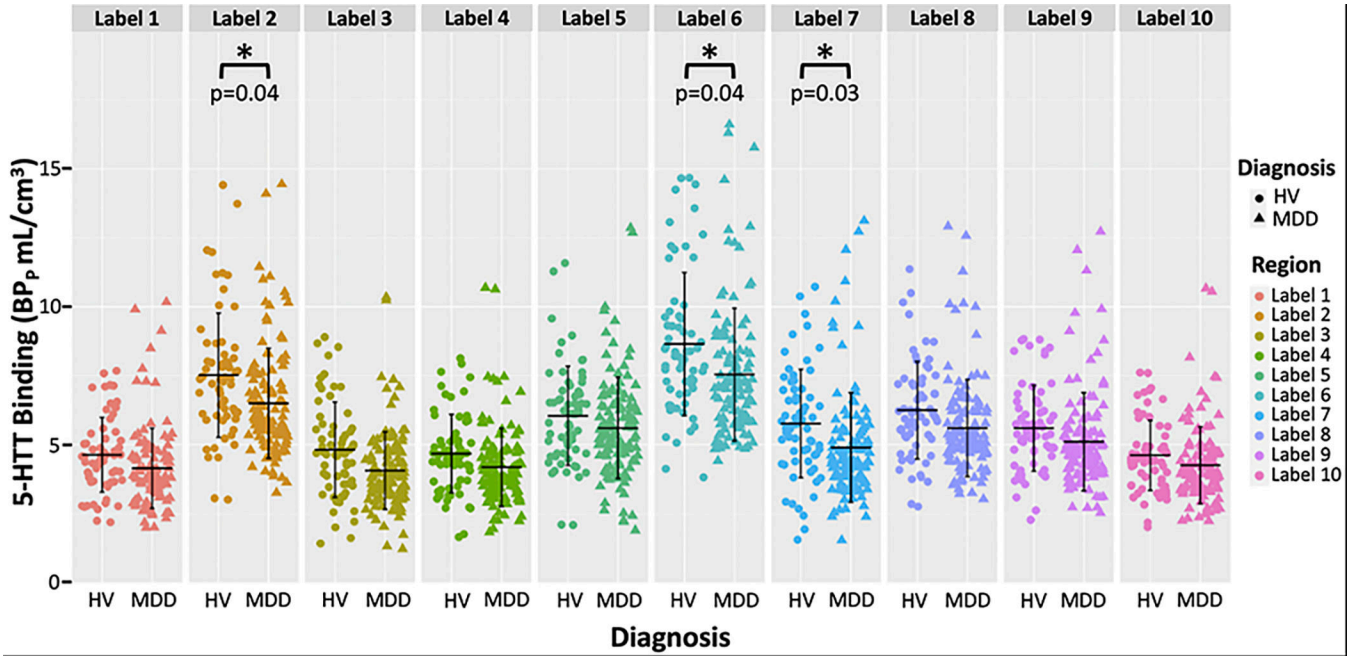


**Figure 4:** Displaying the estimated lower 5-HTT binding potential in MDD relative to the HV group found within the NRU 5-HT Atlas, where 5-HTT binding potential (BP<sub>p</sub>) is plotted for all regions in the NRU 5-HT Atlas, broken down by diagnosis (HV=healthy volunteer with circles, MDD = major depressive disorder with triangles) (top). Regions with p<0.05 in post hoc analysis denoted with \* and p-value is shown. The color-coding for each region in the top graph matches the corresponding region in the NRU 5-HT Atlas shown at bottom with labeling for region number.

**Table 1:**

## MDD and Healthy Volunteer Participant Characteristics

	<b>MDD (n=60)</b>	<b>HV (n=31)</b>	<b>p-value</b>
<b>Age (yrs.)</b>	39.2 ± 11.2	31.7 ± 10.4	p=0.003
<b>% Female</b>	53.3%	51.6%	p=1
<b>% Hispanic</b>	20.0%	9.7%	p=0.26
<b>% Race</b>	75.0% White 6.7% Asian 11.7% Black 5.0% More than one race 1.7% American Indian/Alaskan Native	48.4% White 19.4% Asian 19.4% Black 3.2% More than one race 9.7% unknown/not reported	p=0.02
<b>Years Education</b>	15.6 ± 2.6	16.1 ± 1.9	p=0.27
<b>BDI</b>	22.6 ± 9.9	1.4 ± 2.1	p<0.001
<b>HDRS-17</b>	18.1 ± 4.4	1.2 ± 2.0	p<0.001
<b>SSI Total Score</b>	5.3 ± 6.7	0 ± 0	p<0.001
<b>% Suicide Attempt History*</b>	31.7%	0%	p<0.001
<b>[<sup>11</sup>C]DASB Injected Dose (mCi)</b>	16.2 ± 2.3	16.1 ± 2.4	p=0.92
<b>Lifetime Axis I Disorders</b>		-	-
<b>At least one comorbid Axis I disorder</b>	67.8%	-	-
<b>Generalized anxiety disorder</b>	6.8%	-	-
<b>Post-traumatic stress disorder</b>	18.6%	-	-
<b>Obsessive compulsive disorder</b>	8.5%	-	-
<b>Attention-deficit hyperactive disorder</b>	5.08%	-	-
<b>Panic disorder</b>	10.2%	-	-
<b>Social phobia</b>	16.9%	-	-
<b>At least one lifetime substance use disorder</b>	15.3%	-	-

Abbreviations: BDI = Beck Depression Inventory<sup>32</sup>, HDRS-17 = Hamilton Depression Rating Scale 17-item<sup>64</sup>, SSI = Scale for Suicidal Ideation<sup>35</sup>; data missing from 14 participants, MDD=major depressive disorder, HV=healthy volunteer